7.3 EFFECTS OF ION AND NEUTRON IRRADIATION ON BAM-11 BULK METALLIC GLASS — J. Brechtl[2], N.A.P Kiran Kumar[1], H. Bei[1], and S. J. Zinkle[1,2] (*[1]Oak Ridge National Laboratory, [2]University of Tennessee)*

OBJECTIVE

The goal of this project is to study ion and neutron irradiation effects in BAM-11 bulk metallic glass alloy to determine its viability as a candidate for structural applications in high-radiation fusion environments.

SUMMARY

Bulk metallic glasses are candidates for fusion reactor structural components due in part to their good mechanical properties and near net shape fabrication potential. Metallic glasses might also exhibit good radiation resistance as their amorphous structure prohibits the formation of Frenkel defects, and subsequent voids and dislocation loops. Mechanical properties of $Zr_{52.5}Cu_{17.9}Ni_{14.6}Al_{10}Ti_5$ bulk metallic glass (BAM-11) irradiated with fission neutrons to 0.1 and 1 dpa at ~90°C show a slight increase in the Vickers hardness (roughly ~7, ~10% for 0.1, 1 dpa respectively). Using a Nix-Gao method it was found that the nano-indentation hardness increased by about ~0.4% and ~66% for samples irradiated to 0.1 and 1 dpa. The dynamic Young's modulus in the sample irradiated to 0.1 dpa was ~5% less than the control sample, and the nano-indentation Young's modulus at 0.1, 1 dpa was approximately 1.4%, 0.9% less than the control specimen. The density of BAM-11 decreased roughly ~0.4% for both 0.1 and 1 dpa. The results suggest that the irradiation-induced damage begins to saturate at doses between 0.1 and 1 dpa.

PROGRESS AND STATUS

Introduction

The formation of the first metallic glass of $Au_{75}Si_{25}$ was reported by Duwez at Caltech, USA, in 1960 [1]. More recently, bulk metallic glasses have been proposed as a candidate for use in radiation environments due to their lack of crystalline structure, which prohibit the formation of Frenkel pairs and dislocation loops [2] and might lead to superior resistance to radiation-induced property degradation. Bulk metallic glasses also exhibit exceptional hardness, high strength and corrosion resistance [3].

Another factor which may make amorphous metals desirable is their potentially high helium permeability due to their large free atomic volume and lack of grain boundaries which can act as helium traps [4]. The trapping of helium at defects is very important in irradiated materials since it can lead to embrittlement and swelling. Furthermore, there is some evidence that the amount of retained displacement damage can be significantly less in amorphous materials [5,6]. Recent studies also show that metallic glasses may be resistant to cavity swelling, and hence possibly tritium retention, as compared to crystalline materials, which would make them appealing for fusion energy applications [6, 7]

For this study the neutron irradiation effects on the mechanical properties of bulk metallic glass BAM-11 (composition: $Zr_{52.5}Cu_{17.9}Ni_{14.6}Al_{10}Ti_5$) were investigated. Specimens were irradiated with fission neutrons to 0.1 and 1 dpa at ~90°C.

Experimental Procedures

A $Zr_{52.5}Cu_{17.9}Ni_{14.6}Al_{10}Ti_5$ alloy (BAM-11) was fabricated by arc melting in an argon atmosphere using a mixture of base metals with the following purities: 99.5% Zr, 99.99% Cu, 99.99% Ni, 99.99% Al, and 99.99% Ti. The alloy was then remelted and drop cast in a Zr-gettered helium atmosphere. Specimens were then prepared from the as-cast rods by electrical discharge machining. Table 1 shows the experimental matrix for the current project which includes the testing property, the measurement condition, and the specimen dimension. Samples were encased in a perforated rabbit irradiation capsule which allowed the coolant water to directly contact the samples. Furthermore, the BAM-11 samples were wrapped in aluminum foil to minimize any potential corrosion or contamination.

After encapsulation, BAM-11 specimens were irradiated with fission neutrons at the ORNL High Flux Isotope Reactor (HFIR) in hydraulic tube 2 (HT-2). Here the samples were exposed to neutron fluences of 1.40 X 10^{20} n/cm^2 and 1.35 X 10^{21} n/cm^2 (E>0.1 MeV) in a perforated hydraulic rabbit capsule. Using a conversion factor of ~0.8 dpa per 10^{21}n/cm^2, the neutron doses in the BAM-11 were approximately 0.1 dpa and 1 dpa [8]. The specimens were wrapped in aluminum foil and the external surface of the wrapped specimens was directly exposed to the reactor coolant water at ~60°C. After consideration of internal nuclear heating effects in the samples, the estimated average sample temperature is ~90 ^{o}C.

Table 1. Testing matrix for control samples and after irradiation to 0.1 and 1 dpa at ~ 90°C.

Testing Property	Measurement Condition	Specimen Dimensions
Bulk Hardness (Hv)	At Room Temperature	3 x 2 x 14 mm Ø 3 x 0.4 mm
Nano-indentation Hardness (GPa)	At Room Temperature	3 x 2 x 14 mm Ø 3 x 0.4 mm
Dynamic Young's Modulus (GPa)	At Room Temperature	3 x 2 x 27 mm
Density (g/cm^3)	At Room Temperature	3 x 2 x 27 mm 3 x 2 x 14 mm

Bulk hardness measurements were performed at room temperature using a Buehler Micromet 3 hardness indenter equipped with a Vickers indenter tip. The tests were performed using a 500 g load with a dwell time of 15 s for all indents. Five indents were taken on each specimen to a depth of ~6.5 μm and spaced 500 μm apart. For this experiment both a bend test bar and a transmission electron microscopy (TEM) disk were used. Prior to indentation, both specimens were surface polished with 1 micron diamond lapping film. With respect to the bend test bar, all indents were made on the end regions of the specimen, well away from the center region of the specimen so that later flexural strength tests are not influenced.

Nano-indentation hardness and Young's modulus measurements were performed at room temperature using an Agilent G200 Nano-indenter with a Berkovich diamond indenter tip. Like the Vicker's hardness tests, the samples consisted of a bend test bar and a TEM disk. All the tests were performed in continuous stiffness measurement mode with a constant loading rate $\dot{P}/P = 0.05\text{s}^{-1}$. In total, 20 indents were made where hardness was measured as a function of depth from the point of contact of the nanoindenter with the surface to a depth of about 800 nm. The hardness data below a depth of ~300 nm from the specimen surface was discarded due to large data scatter associated with surface roughness. Hardness was calculated using the Oliver and Pharr method [9, 10]. The area function of the tip in addition to the machine stiffness for the nanoindenter was calibrated by indenting on a standard fused silica sample [2, 11].

Dynamic elastic modulus measurements were performed using the Resonant Frequency and Damping Analyzer (RFDA) from Integrated Material Control Engineering (IMCE). Here two nodes were set up perpendicular to the length and are located 0.224 times the length in from the ends of the specimen. For the experiment the center of the sample was struck. The resultant vibration propagates through the sample where it is absorbed by a transducer located at the end of the sample. The transducer converts the energy of the vibration into a signal which may be analyzed by an oscilloscope.

Density measurements were performed at room temperature using an immersion density instrument, which consists of an ultra-sensitive balance, the Satorius ME215S, a density kit, and a high-precision

digital thermometer. Samples were immersed in a 3M Fluorinert™ Liquid FC-43 which has high density, low surface tension, low thermal expansion, low vapor pressure and low water/air solubility. Each specimen was measured three times and the density was determined using Archimedes principle.

Mechanical Properties

Vickers hardness values of the neutron irradiated BMG specimens are shown in Figure 1. There was a modest increase of ~7% and ~10% at neutron doses (~90 ^{o}C) of 0.1, 1 dpa respectively. Furthermore, the hardness appears to approach saturation for doses above approximately 0.1 dpa. This result is further supported by an earlier study conducted by Perez-Bergquist et al. which irradiated BAM-11 alloy with 3 MeV Ni^{+} ions to doses of 1, 10 dpa [12]. They found that the irradiation induced change in the hardness of the BMG did not change markedly between doses of ~1 and 10 dpa.

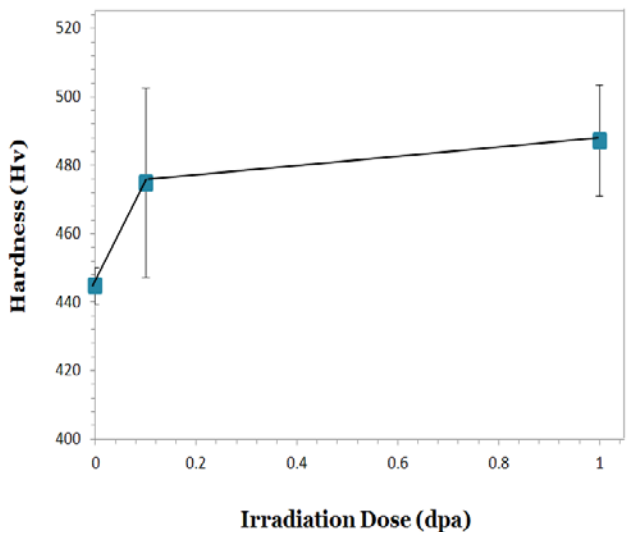

Figure 1. Bulk hardness of neutron irradiated bulk metallic glass samples as a function of irradiation dose.

Nano-indentation hardness was measured as a function of depth from the point of contact of the nano-indenter with the surface to a depth of about 800 nm. The hardness data below a depth of ~300 nm from the specimen surface was discarded due to large data scatter associated with surface roughness. The depth-dependence hardness values of the neutron irradiated BMG specimens are shown in Figure 2. A pronounced depth dependence was measured for the nanoindentation hardness, particularly for the unirradiated and 0.1 dpa irradiated samples. At 800 nm, there was a decrease in the nano-indentation hardness of about ~6% and ~12% from the unirradiated state was observed in the specimens irradiated to 0.1 dpa and 1 dpa.

The as-measured nanoindentation hardness softening implied by Figure 2 is unexpected since the nano-indentation hardness should have a similar trend to the bulk Vickers hardness. It is notable in Figure 2 that the nanoindentation hardness exhibits a pronounced depth dependence. Since the nano-indentation hardness is performed at relatively shallow depths compared to the bulk Vickers hardness measurements (<1 microns vs. ~6.5 microns), the discrepancy between the two hardness tests could be a result of surface effects due to machining or mechanical polishing effects, or a near-surface composition gradient due to chemical inhomogeneity or near-surface radiation induced solute segregation.

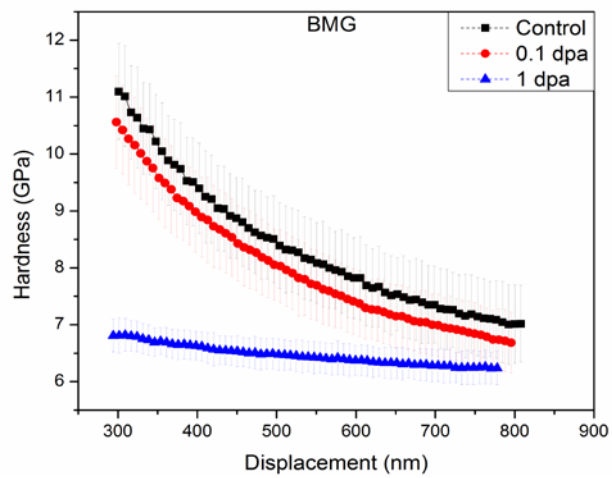

Figure 2. Nano-indentation hardness as a function of indenter depth in the irradiated and control BAM-11 specimens.

In order to make a quantitative comparison of the nano-indentation hardness results with the bulk hardness, the Nix-Gao model was used to evaluate possible near-surface layer with a different hardness than the bulk, and to obtain an extrapolated value of the bulk hardness [13]. For this method, the square of the nano-indentation hardness was plotted vs. the reciprocal of the indentation depth. Samples with uniform hardness should exhibit a linear relationship in this type of plot. To determine the extrapolated bulk hardness H_0, a line was fit to the data and extrapolated towards the ordinate axis. The hardness H_0 occurs where the abscissa equals zero and corresponds with the hardness at an arbitrarily large depth in the material. Due to the deviation away from linear behavior, only the data at a depth >400 nm was used to determine the extrapolated bulk hardness H_0. The extrapolated bulk hardness for each irradiation condition can be seen in Figure 3 below.

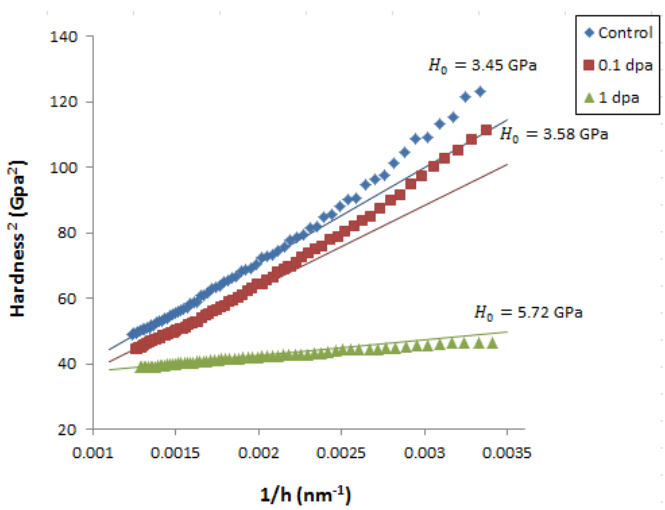

Figure 3. Hardness squared vs. the inverse of the nano-indentation depth.

The hardness results for the hardness H_0 vs. irradiation dose can be seen in Figure 4 below. As can be observed in the graph, the hardness results for the Nix-Gao model exhibits a similar qualitative trend as the Vicker's bulk hardness in the material (Figure 1). In particular, the extrapolated bulk hardness derived from a Nix-Gao analysis indicates an increase of ~0.4%, ~66% after irradiation to 0.1 and 1 dpa, respectively as compared to the unirradiated specimen. The results suggest that there may be a surface

modification which affects the surface hardness of the BAM-11 alloy which may require further investigation, including nanoindentation to deeper depths.

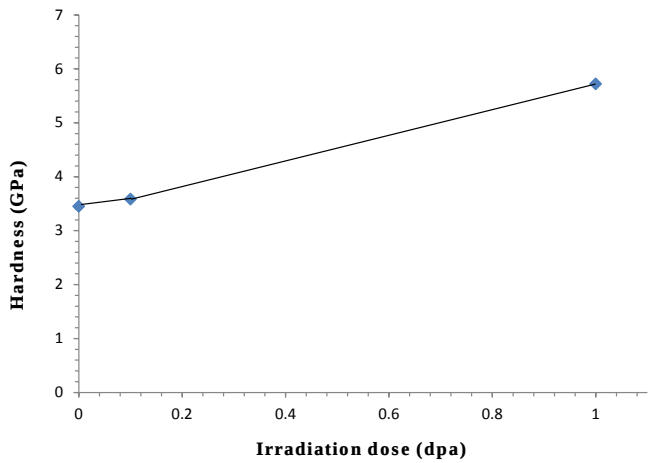

Figure 4. Nix-Gao extrapolated bulk hardness vs. irradiation dose.

The Young's modulus vs. nano-indentation depth can be seen in Figure 5 below. As can be seen, the elastic modulus decreases with increasing depth, resembling the trend for nano-indentation hardness. At 800 nm, the data indicates a slight decrease of ~1.4% and ~0.9% after irradiation to 0.1 and 1 dpa, respectively as compared to the unirradiated specimen

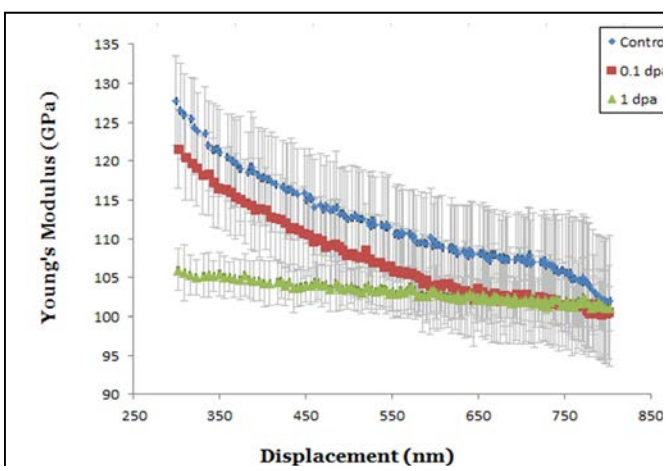

Figure 5. Young's modulus vs. nano-indentation depth.

The dynamic Young's modulus for the control and sample irradiated to 0.1 dpa can be seen in Table 2 below. There was a decrease of ~5% in the dynamic Young's modulus of the specimens irradiated to 0.1 dpa at 90°C as compared to the control sample.

An experiment conducted by Perez-Bergquist et al., which involved the Ni^+ ion irradiation of the same BAM-11 bulk metallic glass at room temperature and 200 ^{0}C, observed different responses in the nano-indentation hardness and Young's modulus [2]. Specifically, it was found that samples irradiated at room temperature exhibited a clear drop in hardness and elastic modulus while samples irradiated at 200 ^{0}C did not experience significant changes in hardness and saw only small changes in Young's modulus.

Table 2. Average dynamic Young's modulus of unirradiated and irradiated BMG specimens.

BMG	Control	0.1 dpa – 90°C
Average Dynamic Young's Modulus (GPa)	79.4	75.7
Std. Dev of Dynamic Young's Modulus (GPa)	0.7	1.8

However, the results of the Vicker's bulk hardness and the Nix-Gao analysis for nano-indentation hardness indicate that bulk metallic glasses exhibit increased hardness when exposed to neutron irradiation up to doses in the range of 0.1 and 1 dpa. The moderate quantitative discrepancies between the Nix-Gao extrapolation and the Vicker's hardness results require further investigation.

The measured densities for the control and irradiated specimens are listed in Table 3. A decrease in density was found in the irradiated samples as compared to the control specimens. Here the specimens exhibited ~0.4% decrease in density at both irradiation doses. Moreover, the density at 1 dpa was slightly greater than the density at 0.1 dpa. The slight change in density is likely associated with the irradiation induced rearrangement of short range atomic bonding which results in greater atomic spacing.

Previous studies have also found neutron irradiation induced microstructural changes in metallic glasses. For example, a study conducted by Gupta et al. found that thermal neutron irradiation of iron based metallic glass to low doses increased the short range order which was accompanied by a relief in the random internal stresses of the as received specimens [14]. In contrast to the above studies, the study by Perez-Bergquist et al. found no significant microstructure changes of BAM-11 after exposure to Ni^+ ion irradiated BAM-11 [2]. This discrepancy between experimental results of ion and neutron irradiation warrants further research on the radiation response of BAM-11 amorphous alloy.

Table 3. Measured density of unirradiated and irradiated BMG specimens

Condition	Specimen weight (g)		Density of specimen (g/cm^3)
	In Air	In Fluid	
Control	0.98818	0.70871	6.66046
0.1 dpa	1.06142	0.76024	6.63491
1 dpa	1.06797	0.76475	6.63520

In summary, there were relatively slight irradiation induced changes in the bulk hardness, nano-indentation hardness, density and dynamic Young's modulus for the given dose regime. For the first three tests, the exhibited change did not differ significantly between the samples tested at 0.1 and 1 dpa. This result signifies that a saturation of irradiation damage may be occurring in BAM-11 within the examined dose regime.

Conclusions

After irradiation with fission neutrons to dose levels of 0.1 and 1 dpa at ~90 ^oC, the BAM-11 bulk metallic glass specimens were found to exhibit slight decreases in both the dynamic and nanoindentation Young's modulus. Specifically there was a drop of 5% for the dynamic Young's modulus at 0.1 dpa while for the nano-indentation Young's modulus there was a drop of 1.4% and 0.9% for 0.1 and 1 dpa respectively. The density was found to drop by 0.4% for both irradiation conditions, which suggests BAM-11 is susceptible to a slight neutron induced densification. In terms of hardness, there was an 7-10% increase in the bulk hardness and a 0.4%, 66% increase in the nano-indentation hardness based on a Nix-Gao extrapolation of the data. In addition, damage approaching a dose of approximately 1 dpa exhibits an apparent saturation based on the results of the density and bulk Vickers hardness tests.

In summary, the material response of BAM-11 following fission neutron irradiation indicates that the alloy exhibits good resistance to pronounced structural and property changes during low dose neutron irradiation near room temperature. However, further studies of the bulk metallic glass are needed to fully understand the effects of neutron irradiation on the material. These studies include Transmission Electron Microscopy (TEM) and Extended X-ray Absorption Fine Structure (EXAFS) to explore nanoscale changes to microstructure, if any. Future experiments may include neutron irradiation to doses of ~10 dpa and ion irradiation to doses greater than 10 dpa to examine whether BAM-11 exhibits a true saturation effect.

References

[1] W. Klement, R.H. Wilens, and P. Duwez, Nature, 187 (1960) 869-870.

[2] A. G. Perez-Bergquist, H. Bei, K. J. Leonard, Y. Zhang, S. J. Zinkle,. Intermetallics 53 (2014) 62-66.

[3] A. Inoue, Acta Materialia, 48 (2000) 279-306.

[4] W.J. Weber, R.C. Ewing, C.A. Angell, G.W. Arnold, A.N.Cormack, J.M. Delaye, D.L. Griscom, L.W. Hobbs, A.Navrotsky, D.L. Price, A.M. Stoneham, and M.C. Weinberg, J. Mater. Res. 12 (1997) 1946 – 1978.

[5] W.J. Weber, R.C. Ewing, C.A. Angell, G.W. Arnold, A.N. Cormack, J.M. Delaye, D.L. Griscom, L.W. Hobbs, A. Navrotsky, D.L. Price, A.M. Stoneham, and M.C. Weinberg, J. Mater. Res.12 (1997) 1946-
1978.

[6] A. G. Perez-Bergquist, H. Bei, Y. Zhang, and S.J. Zinkle, Fusion Materials Semiannual Progress Report for Period Ending December 31, 2013, DOE/ER-0313/26, U. S. Department of Energy, 154.

[7] X. Mei, B. Wang, C. Dong, F. Gong, Y. Wang, and Z. Wang, Nucl. Instrum. Methods Phys. Res. B
307(2013) 11-15.

[8] L.L. Snead, J. Nucl. Mater., 326 (2004) 114-124.

[9] W.C. Oliver and G.M. Pharr, J. Mater. Res. 7 (1992) 1564-1583.

[10] W.C. Oliver and G.M. Pharr, J. Mater. Res. 19 (2004) 3-20.

[11] W. Li, H. Bei, Y. Tong, W. Dmowski, and Y.F. Gao, Appl. Phys. Lett. 103 (2013) 171910.

[12] A. G. Perez-Bergquist, J. Brechtl, H. Bei, Y. Zhang, and S. J. Zinkle, Fusion Materials Semiannual Progress Report for Period Ending June 30, 2014, DOE/ER- 0313/56, U.S. Department of Energy, 184.

[13] W.D. Nix and H. Gao, J. Mech. Phys. Solids, 46, (1998) 411-425.

[14] A. Gupta and S. Habibi, Mat. Sci. and Engineering A134 (1991), 992-995.